

Disposition of water in chloroplast coupling factor 1 (CF₁)

A neutron scattering analysis

Konrad Ibel*, Siegfried Engelbrecht, Richard Wagner, Carlos S. Andreo⁺ and Wolfgang Junge

*Universität Osnabrück, Biophysik, Barbarastr. 11, D-4500 Osnabrück, FRG and *Institut Max von Laue-Paul Langevin, 156X, F-38042 Grenoble Cedex, France*

Received 26 April 1989

Small-angle neutron scattering experiments were performed in dilute aqueous solutions of chloroplast F₁-ATPase. By contrast variation in ¹H₂O/²H₂O mixtures and when using different concentrations of glycerol in ²H₂O, structural information on the spatial distribution of dry protein and water was obtained. The maximum distance within latent and active CF₁ was 12 nm. The shape of CF₁ was globular. The total volume of CF₁ was 900 nm³, and its dry volume (excluding the volume of one water molecule per two exchangeable hydrogen atoms) was 400 nm³. A volume of 670 nm³ was inaccessible to glycerol at low glycerol concentrations (less than 25%). At higher concentrations (up to 50%) a volume of 460 nm³ was excluded to glycerol. Within the resolution of our experiment (1.6 nm) there was no evidence for particular water-rich regions or of secluded water spaces or any particular places for glycerol exchange. Upon thiol activation of the latent enzyme only small changes in structure were detectable just at the limits of the experimental error. They suggest an enhancement of the surface roughness.

ATPase; Water structure; Enzyme activation; Neutron scattering; Photosynthesis

1. INTRODUCTION

H⁺-ATPases play a key role in bioenergetics of the living cell. ATP is synthesized by the membrane-bound F₀F₁ complex which uses the difference between the electrochemical potential of the proton across the coupling membrane. H⁺-ATPases consist of the membrane-embedded F₀ portion and the soluble F₁ part which is external to the membrane. F₀ serves as a proton conductor. In chloroplasts, it consists of four types of subunits. The soluble part F₁ carries the catalytic centers. It consists of five subunits termed α , β , γ , δ and ϵ in order of decreasing molecular masses (55 462, 53 874, 34 500, 20 468 and 14 700 Da,

respectively). The subunits are combined in a 3:3:1:1:1 stoichiometry (review [1]).

Biochemical and biophysical investigations revealed that the soluble part CF₁ exists in two functional and structural states [2]. In the latent state, 500–600 hydrogen atoms are bound in nearly nonexchangeable manner to the interior of CF₁ [3]. The physiological significance of the latent state possibly lies in the suppression of ATP hydrolysis in the absence of driving force, e.g. during night. In vivo, activation is a two-step process: First, it is brought about by membrane energization, then reduction of a disulfide bridge in the γ -subunit occurs by means of the thioredoxin system [4]. The latter can be achieved, e.g. by thiol treatment [5]. Interestingly, mitochondrial and bacterial H⁺-ATPases only exist in the active state.

The structural difference between the latent and the activated, reduced state of CF₁ was also apparent from changes in the hydrodynamic properties. A drastic increase in the rotational diffusion

Correspondence address: K. Ibel, Institut Laue-Langevin, 156X, F-38042 Grenoble Cedex, France

⁺ *Permanent address:* Centro de Estudios Fotosintéticos y Bioquímicos, Suipacha 531, 2000 Rosario, Argentina

correlation time by about 300% after dithioerythritol activation of latent CF₁ has been reported by Wagner et al. [6] while Schinkel and Hammes [7] observed a slight decrease (~15%).

As another indication for a structural change we have used the triplet lifetime of eosin which was covalently attached to CF₁. This lifetime depends on the accessibility of the dye for O₂. The lifetime was much longer in the latent than in the active state [8]. This finding and the relatively high rotational freedom of the labels led to the conclusion that latent CF₁ may contain a sequestered solvent space which, upon activation of CF₁, gains accessibility to the surrounding medium [6]. Viale et al. [2] drew similar conclusions before from hydrogen exchange studies with latent and activated CF₁.

The most direct methods for investigating structures on the molecular level are the diffraction techniques. Small-angle neutron scattering experiments have been performed with solutions of *E. coli* ATPase [9]. In heavy water, ²H₂O, a globular shape was observed. Neutron scattering results on CF₁ have also been obtained recently by Calmettes et al. [10]. They studied CF₁ under different conditions in heavy water and observed a globular shape as well. The structure turned out to be insensitive to activation.

Neutron scattering has the specific advantage that the structure of hydrogen atoms can be investigated due to the different scattering sensitivity of neutrons to protonated hydrogen, ¹H, and to the hydrogen isotope deuterium, ²H. The contrast variation by using buffers with different proportions of heavy water, ²H₂O, to light water, ¹H₂O, is especially useful in the structure analysis of complex biological systems if these complexes are composed of portions with chemically different material or of portions which are specifically deuterated [11].

The differences between the latent and active state, as described above, are intimately connected with differences in the disposition of water within the enzyme complex. However, neutron scattering using ¹H₂O/²H₂O contrast variation is unable to discriminate between loose water molecules and those which are bound to the external and internal hydrophilic surfaces of protein complexes. Since glycerol is a small organic molecule which cannot easily penetrate into the layers of bound water

around hydrophilic proteins, additional measurements were performed in the presence of different glycerol concentrations in the heavy water buffer.

Contrast variation using small organic molecules has been used by Stuhmann et al. for investigating the structure of apoferritin [12]. Further experiments specifically aimed at the structure of water-rich regions in chromatin core particles [13] and at the structure of the shell of bound water in ribonuclease A [14]. In both cases the water could be localized unambiguously at the exterior of the solute particles.

The present study aimed at the analysis of the partial structures of water and of dry protein, as well as of structural changes occurring during the transition from the latent to the active state.

2. MATERIALS AND METHODS

CF₁ was purified from spinach thylakoids as described [15,16]. It was gel-filtered through disposable PD-10 columns (Pharmacia) equilibrated with 50 mM Tris-HCl (pH 7.8), 2 mM EDTA, 1 mM ATP and 10% glycerol buffer just before the beginning of the neutron scattering experiments. DTT activation of CF₁ was performed as in [2]. Protein concentrations were determined according to Sedmak and Grossberg [17] using ovalbumin as standard. All reagents used here were of analytical grade.

The neutron camera was instrument D11 at the High-Flux Reactor of the Institut Laue-Langevin, Grenoble [18]. The wavelength used for the experiments was 1.0 nm; the sample-to-detector distances were 1.1 and 4.0 m. Sample solutions were contained in quartz cells of 1.00 mm optical path length; the irradiated volume was 229 μl. Protein concentrations were between 1.9 and 2.5 mg/ml. The attenuation T_s of the primary beam was taken into account for determining the coherent differential scattering cross-section per particle,

$$\frac{d\sigma(Q)}{d\Omega} = \frac{I_s(Q)}{I_0 \Delta\Omega T_s n d}$$

with $I_s(Q)$, the intensity scattered by sample and d , the thickness of sample.

$$Q = \frac{4\pi}{\lambda} \sin \frac{\vartheta}{2}$$

is the momentum transfer, with λ , the neutron wavelength and ϑ , the full scattering angle. The value $M_r = 408\,000$ was used for calculation of the number densities of the particles,

$$n = \frac{c N_A}{M_r}$$

with c denoting the mass density of the solute and N_A , Avogadro's number. The purely incoherent, hence isotropic, scattering of a (light) water sample of 1.00 mm thickness [19] was used for calibrating the product of the intensity I_0 of the

primary beam and the solid angle $\Delta\Omega$ subtended by the detection elements.

The differential scattering cross-sections can be transformed into pair distance distribution functions $P(R)$. These functions indicate the probability of finding a pair of scattering centers of mutual distance R , multiplied by their respective excess scattering lengths. We used the indirect Fourier transformation method of Glatter [20]. The differential scattering cross-section per particle at zero momentum transfer, i.e. the integral of $P(R)$, was also obtained by this procedure.

3. RESULTS AND DISCUSSION

The soluble part of the proton-translocating ATPase of spinach chloroplasts is a multi-subunit enzyme complex. We were interested in the disposition of water within this complex and also in the structure before and after thiol activation. Neutron small-angle scattering experiments were carried out with dilute solutions in buffers containing volume fractions of heavy water [0, 12.5, 25, 37.5, 50 and 100% (v/v)], as well as with solutions in heavy water buffers containing different amounts of glycerol [0, 12.5, 25, 37.5 and 50% (v/v)] which was deuterated at the labile sites.

All measurements were performed first with latent CF₁ and repeated after 3 h incubation with dithioerythritol (50 mM). This experimental approach reduced any possible systematic errors of relative changes in intensity to a minimum. The neutron scattering data (fig.1) showed no appreciable changes upon activation, within the resolution of

$$\pi/Q_{\max} = 1.6 \text{ nm}$$

Only in ²H₂O and at momentum transfers beyond $Q = 0.8 \text{ nm}^{-1}$ was the scattering of activated CF₁ (fig.1) almost 15% stronger than that of latent CF₁ (fig.1). This difference, however, is not appreciably larger than the assumed experimental error.

In measurements of the rotational diffusion of isolated CF₁ the rotational correlation time of the enzyme increased drastically (3-fold) after DTT activation [6]. A recent reinvestigation of this matter, however, indicated only an increase of 12% in the rotational correlation time upon DTT activation of CF₁ (320 ± 8 vs 360 ± 6 ns; Apley, E.C., unpublished). The previously observed larger increase in the rotational correlation time was probably due to aggregations in these samples.

The observed change could be related to a pro-

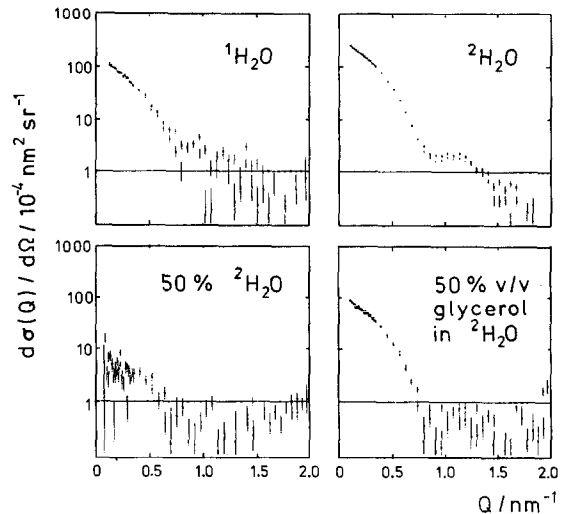


Fig.1. Neutron small-angle differential scattering cross-section per latent particle (+) and activated particle (x). (Upper left) 100% ²H₂O buffer; (upper right) in ¹H₂O buffer; (lower left) in 50% (v/v) glycerol/²H₂O buffer; (lower right) in 50% ¹H₂O/50% ²H₂O buffer. Scattering data obtained at intermediate concentrations (now shown) exhibit, within statistical deviations and experimental errors, identical shapes of angular distributions.

portional increase in the hydrodynamic volume of CF₁. The suggested increase in the neutron scattering cross-section at relatively large scattering angles upon DTT activation of CF₁ is also compatible with an increase in hydrodynamic volume because it may reflect an increase in surface roughness [21]. Since the scattering remained unchanged at $Q \leq 0.8 \text{ nm}^{-1}$, an increase or decrease of intersubunit distances of more than $\sim 2\%$ could be excluded.

Another aim of our experiments was to investigate the structure of sequestered and externally bound water, that of the 'dry' protein, and the mutual disposition of these two moieties. To this end we performed contrast variation experiments in heavy water which contained different amounts of deuterated glycerol.

Fig.1 shows that the shape of the scattering curves of latent and activated CF₁ was not subject to appreciable changes when observed at different scattering length densities of the buffer. The results obtained with ¹H₂O, ²H₂O, 50% ¹H₂O/50% ²H₂O and 50% (v/v) glycerol in ²H₂O were confirmed by the scattering data obtained at intermediate buffer densities (not shown).

The square root of the differential scattering cross-section per particle at zero momentum transfer depended, in the case of $^1\text{H}_2\text{O}/^2\text{H}_2\text{O}$ contrast variation, linearly on the scattering density of the buffer (fig.2). The slope of the straight solid line yields that volume occupied by the dry protein mass ($400 \pm 20 \text{ nm}^3$) which excludes the protonated and deuterated hydrogen atoms of the buffer. The so-called 'dry volume' of the complex, which includes the volume 0.030 nm^3 to be assigned to two sites of exchangeable hydrogens, is usually assumed to be about 20% larger than the 'invariant' volume observed with $^1\text{H}_2\text{O}/^2\text{H}_2\text{O}$ contrast variation [11]. With 6500 labile hydrogen atoms [10] we calculate a dry volume of 490 nm^3 .

Plots of the square root of the differential scattering cross-section per particle at zero momentum transfer vs the scattering density of the glycerol-

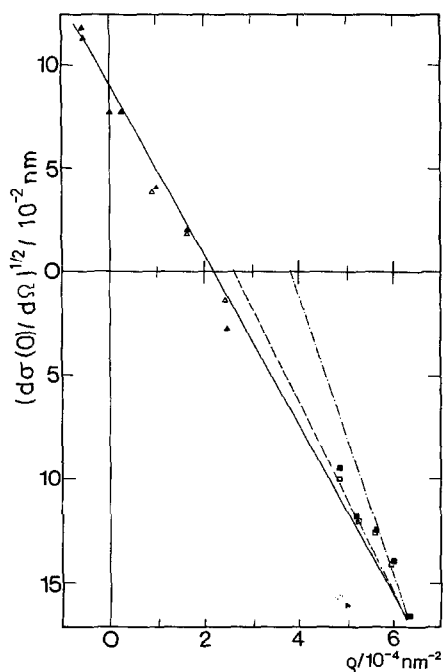


Fig.2. Square roots of scattering cross-sections per particle at zero momentum transfer ($d\sigma(\phi)/d\Omega$) vs scattering density of the buffer. The ordinate values were taken from the extrapolated data shown in fig.1. $^2\text{H}_2\text{O}$ concentrations: 0, 12.5, 25, 37.5, 50% (v/v) (triangles) and 100%. Glycerol concentrations: 0, 12.5, 25, 37.5, 50% (v/v) (squares). Filled symbols show data obtained with the latent state and empty symbols those for the activated state. The slopes of the straight lines give the volumes of the particle which are excluded from the contrasting medium ($^1\text{H}_2\text{O}/^2\text{H}_2\text{O}$ and glycerol, respectively).

water mixtures are shown in fig.2, lower right corner. The slope of the dashed-dotted line yielded the volume, $670 \pm 40 \text{ nm}^3$, occupied by the hydrated particle which is not accessible to glycerol molecules, at glycerol concentrations $\leq 25\%$ (v/v). This excluded volume decreased to 460 nm^3 when the glycerol concentration exceeded 30% (v/v). Within the error limits, this value is identical to the dry volume as calculated above. A similar dehydrating effect can be read from the data obtained with chromatin core particles [13].

The angular distribution of the differential scattering cross-section per particle allowed for calculation of the pair distance distribution functions for each ($^1\text{H}_2\text{O}/^2\text{H}_2\text{O}$ and glycerol) contrast [20]. These distribution functions are bell-shaped as expected for homogeneous globular particles. The diameter obtained from the data is $12 \pm 0.5 \text{ nm}$. The corresponding volume of 900 nm^3 was very similar to the volume of the latent enzyme determined using hydrodynamic methods [6].

The degree of hydration of soluble CF_1 could be calculated from the difference between the hydrodynamic volume and the volume excluded to glycerol at relatively high concentrations to be $0.6 \text{ g H}_2\text{O/g CF}_1$ (14700 water molecules per en-

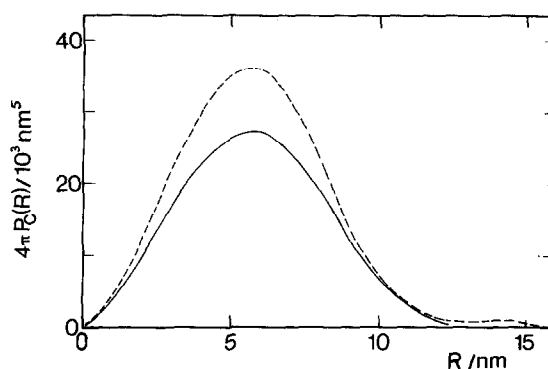


Fig.3. Pair distance distribution functions of volume elements which are both situated within the volume which is not accessible for the medium used for contrast variation. The ordinate scale is normalised to give $4\pi \int P_c(R)dR$ in nm^6 , i.e. the square of the excluded volume. Solid line: $^1\text{H}_2\text{O}/^2\text{H}_2\text{O}$ contrast variation; dashed line: glycerol contrast variation at high glycerol concentrations (the pair distance distribution function at low glycerol concentrations shows within the same shape a further increase in the ordinate values). The distributions indicate a globular shape of the particles. The part of the curve which is situated beyond $R = 12 \text{ nm}$ probably reflects a moderate aggregation induced by glycerol.

zyme complex). Our results show that slightly more than half of the water was loosely bound and easily removed by addition of glycerol. The remaining fraction was more firmly bound. It could be removed by high glycerol concentrations only.

The data gave the fundamental pair distance distribution functions [22]: $P_s(R)$ is independent of the contrast, $\bar{\rho}P_{cs}(R)$ is linearly dependent on the contrast $\bar{\rho}$ between the mean scattering length density of the particle and the scattering length density of the buffer; $\bar{\rho}^2P_c(R)$ is proportional to the square of the contrast. Fig.3 shows $4\pi P_c(R)$, which is the quadratic term after normalization to the square of the contrast, for $^1\text{H}_2\text{O}/^2\text{H}_2\text{O}$ contrast variation (solid line) and for glycerol contrast variation at high glycerol concentration (dashed line). The term $P_s(R)$, which is due to internal fluctuations of the scattering length density is indistinguishable from zero, both within the invariant volume occupied by the protein as well as within that occupied by the hydrated particle, i.e. the glycerol-inaccessible volume. Therefore, within the limits of resolution of our experiments, the sites of exchangeable hydrogen atoms and of bound water are homogeneously distributed throughout the hydrodynamic volume occupied by the molecule.

Our data are in accordance with the density maps from a crystallographic investigation [23]. They show at low resolution a quite uniform distribution of protein within the unit cell, i.e. they seem to exclude the existence of a large continuous solvent space. The dehydrating effect of glycerol at high concentration possibly produces small conformational changes of the protein polypeptide chains by removal of water from channels and small pockets.

Acknowledgements: This work was supported by Bundesministerium für Forschung und Technologie (FKZ 03-B63 A 47). Preparation of the figures by H. Kenneweg is acknowledged.

REFERENCES

- [1] Senior, A.E. (1988) *Physiol. Rev.* 68, 177-231.
- [2] Viale, A., Vallejos, R. and Jagendorf, A.T. (1981) *Biochim. Biophys. Acta* 637, 496-503.
- [3] Mills, J.D., Mitchell, P. and Schürmann, P. (1980) *FEBS Lett.* 112, 173-176.
- [4] Nalin, C.M. and McCarty, R.E. (1984) *J. Biol. Chem.* 259, 7275-7280.
- [5] Arno, J.H. and Vallejos, R.H. (1982) *J. Biol. Chem.* 257, 1125-1127.
- [6] Wagner, R., Engelbrecht, S. and Andreo, C.S. (1985) *Eur. J. Biochem.* 147, 163-170.
- [7] Schinkel, J.E. and Hammes, G.G. (1986) *Biochemistry* 25, 4066-4071.
- [8] Wagner, R., Andreo, C.S. and Junge, W. (1983) *Biochim. Biophys. Acta* 723, 123-127.
- [9] Satre, M. and Zaccai, G. (1979) *FEBS Lett.* 102, 244-247.
- [10] Calmettes, P., Girault, G., Berger, G. and Galmiche, J.M. (1989) *Physica B*, in press.
- [11] Ibel, K. and Stuhmann, H.B. (1975) *J. Mol. Biol.* 93, 255-265.
- [12] Stuhmann, H.B., Haas, J., Ibel, K., Koch, M.H.J. and Crighton, R.R. (1976) *J. Mol. Biol.* 100, 399-413.
- [13] Baldwin, J.P., Braddock, G.W., Carpenter, B.G., Kneale, G.G., Simpson, J.K., Suau, P., Hjelm, R.P. and Bradbury, E.M. (1978) *J. Appl. Crystallogr.* 11, 483-484.
- [14] Lehmann, M.S. and Zaccai, J. (1984) *Biochemistry* 23, 1939-1942.
- [15] Engelbrecht, S., Lill, H. and Junge, W. (1986) *Eur. J. Biochem.* 160, 635-643.
- [16] Apley, E.C., Wagner, R. and Engelbrecht, S. (1985) *Anal. Biochem.* 150, 145-154.
- [17] Sedmak, J.J. and Grossberg, S.E. (1977) *Anal. Biochem.* 79, 544-552.
- [18] Ibel, K. (1976) *J. Appl. Crystallogr.* 9, 269-309.
- [19] May, R.P., Ibel, K. and Haas, J. (1982) *J. Appl. Crystallogr.* 15, 15-19.
- [20] Glatter, O. (1977) *J. Appl. Crystallogr.* 10, 415-421.
- [21] Glatter, O. (1982) in: *Small Angle X-ray Scattering* (Glatter, O. and Kratky, O. eds) pp. 168-169, Academic Press, New York.
- [22] Stuhmann, H.B. and Kirste, R.G. (1984) *J. Appl. Crystallogr.* 7, 173-178.
- [23] Amzel, L.M., McKinney, M., Narayanan, P. and Pedersen, P.L. (1982) *Proc. Natl. Acad. Sci. USA* 79, 5852-5856.